Physics of the Earth and Planetary Interiors 187 (2011) 56–65

Contents lists available at ScienceDirect

Physics of the Earth and Planetary Interiors

journal homepage: www.elsevier.com/locate/pepi

Regional variation in shear-wave polarization anisotropy of the crust in southwest Japan as estimated by splitting analysis of Ps-converted waves on receiver functions

Mamoru Nagaya, Hitoshi Oda *, Tetsuro Kamimoto

Department of Earth Sciences, Okayama University, Okayama 700-8530, Japan

ARTICLE INFO

Article history:
Received 14 July 2009
Received in revised form 11 April 2011
Accepted 23 April 2011
Available online 20 May 2011

Keywords:
Shear-wave polarization anisotropy
Ps-converted wave
Receiver function
Crust
Shear-wave splitting analysis
Southwest Japan

ABSTRACT

Regional variation in shear-wave polarization anisotropy of the crust is investigated in the Kyushu, Chugoku, Shikoku and Kinki districts, southwest Japan, using Ps-converted phases generated at the Moho discontinuity. The Ps phases on radial and transverse receiver functions are analyzed to determine shear-wave splitting parameters of fast polarization direction and time lag by waveform cross-correction analysis. As a result, the fast polarization directions are shown to be obviously different between the Chugoku district and the Kyushu and Shikoku districts, which are separated from each other by the Seto Inland Sea. In the Kyushu, Shikoku and south Kinki districts, the Ps phases exhibit fast polarization directions ranging from E–W to NW–SE. The polarization directions are not only consistent with those of S waves from shallow crustal earthquakes but also parallel to the direction of maximum horizontal compression acting on southwest Japan and the strike directions of metamorphic belts, accretionary zones and rift zones. Thus the polarization anisotropy is understood to reflect mainly the upper crustal anisotropy that is attributable to stress-induced vertical cracks and geological lineament structure. On the other hand, in the Chugoku and north Kinki districts, fast polarization directions are in a range from N–S to NE–SW. They are not consistent with the tectonic stress field and the S-wave splitting observed for shallow crustal earthquakes. The disagreement between the fast polarization directions estimated from the S waves and the Ps-converted phases is interpreted as arising because the lower crustal anisotropy attributed to mineral preferred orientation has a significant influence on the Ps-phase splitting. The regional variation in Ps-phase polarization anisotropy of the crust in southwest Japan is dependent on which anisotropy of the upper and lower crust is prominently reflected in the Moho Ps-phase splitting.

1. Introduction

A shear wave splits into two components due to the elastic anisotropy when propagating through an elastically anisotropic solid. This phenomenon is called shear-wave splitting. Fast component of the split shear wave is polarized nearly parallel to *a*-axis for orthorhombic symmetry and to *c*-axis (hexagonal-symmetry axis) for hexagonal symmetry (e.g., Kasahara et al., 1968; Anderson, 1989). The upper mantle is composed mainly of olivine with orthorhombic symmetry and olivine-rich peridotite with approximately hexagonal symmetry. Furthermore, elastic behavior of the crust which contains a number of faults and cracks is expected to show hexagonal anisotropy. Thus the shear-wave splitting is of benefit to the study of seismic anisotropy of the upper mantle and crust of the Earth (e.g., Ando et al., 1980; Kaneshima, 1990; Nakajima and Hasegawa, 2004; Long and van der Hilst, 2005).

To diagnose seismic anisotropy of the crust, direct S waves from shallow crustal earthquakes are usually analyzed (e.g., Kaneshima, 1990), while SKS and ScS waves are used for the study of mantle anisotropy (e.g., Silver and Chan, 1991; Oda and Shimizu, 1997). A limitation of the methodology is poor resolution in the depth direction of anisotropic structure. In other words, it is difficult to pinpoint where seismic anisotropy exists on the ray path because the effect of anisotropy is reflected in the waveform in the form of signal accumulated along a propagation path of S wave. The shortcoming is mitigated by using P-to-S (Ps) converted phase that originates at a velocity discontinuity interface, because the Ps-converted phase contains information on seismic anisotropy within a zone between the conversion interface and the ground surface. McNamara and Owens (1993) made the first attempt to extract the anisotropic signal from Moho Ps-converted phase by a particle motion analysis. Subsequently shear-wave splitting of the Ps-converted phases was examined in detail using synthetic receiver functions calculated for some anisotropic layer models (Savage, 1998), and the Ps-phase splitting was shown to be useful for the

* Corresponding author. Fax: +81 86 251 7895.
E-mail address: lfee0688@cc.okayama-u.ac.jp (H. Oda).

0031-9201/$ - see front matter © 2011 Elsevier B.V. All rights reserved.
doi:10.1016/j.pepi.2011.04.016

study of crustal anisotropy. Iidaka and Niu (2001) and Iidaka (2003), instead of the Ps phase, recommended using later S phases such as PpPms and PpSms phase, which are reverberated in the crust as a kind of shear wave. But the reverberated S phases might be sometimes difficult to identify on seismic records because of their small amplitudes. Therefore the Ps-converted phases seem to be preferable to the reverberated S phases for detection of the shear-wave polarization anisotropy in the crust.

A recent study on shear-wave splitting analysis of Moho Ps-converted phases indicated that in the Chugoku district fast polarization directions of the Ps phases are within a range of direction from N–S to NE–SW (Nagaya et al., 2008). This range of the directions is basically consistent with the fast polarization directions estimated from PpPms and PpSms waves reverberated in the crust (Iidaka, 2003) and fast propagation directions of P-wave azimuthal anisotropy of the crust (Ishise and Oda, 2008) but inconsistent with fast polarization directions which were estimated by shear-wave splitting analysis of direct S waves from shallow crustal earthquakes (e.g., Kaneshima, 1990; Mizuno and Nakai, 2005). The shear-wave splitting of the Ps phases and the reverberated S waves tells us about an averaged anisotropy over the entire depth of crust, while the splitting of direct S waves from shallow crustal earthquakes informs us of upper crustal anisotropy which is probably governed by the global tectonic stress acting on the Japan Islands arc (Kaneshima, 1991). Thus the disagreement between the fast polarization anisotropy estimated from S waves and other later S phases suggests that there may be some differences in seismic anisotropy between the upper and lower crust. In this paper, we see whether or not the fast polarization directions estimated from the Moho Ps-converted phase are consistent with those estimated from the shear-wave splitting of S waves. For this purpose, the fast polarization directions are estimated in the Shikoku, Kyushu and Kinki districts by shear-wave splitting analysis of the Moho Ps-converted phases identified on receiver functions. The estimated fast polarization directions are plotted on seismic stations, together with the fast polarization data obtained in the Chugoku district (Iidaka, 2003; Nagaya et al., 2008). An entire picture of distribution of the fast polarization directions allows us to discuss feature of the regional variation in the shear-wave polarization anisotropy of the crust. In addition, we address an issue of what influence the difference in seismic anisotropy between the upper and lower crust has on shear-wave splitting of the Moho Ps-converted phase, because the Ps phase is split by both anisotropic regions. Lastly we interpret the regional variation in the estimated polarization anisotropy in connection with the effect of seismic anisotropy of the lower crust.

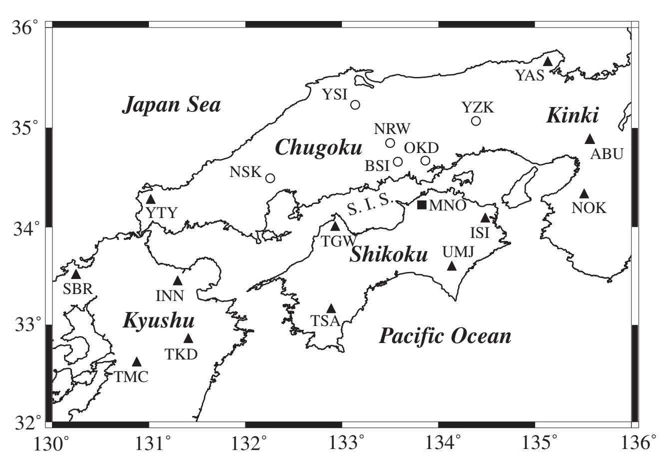

Fig. 1. Locations of seismic stations in the Kinki, Chugoku, Shikoku and Kyushu districts. Open circles indicate seismic stations used in the study of Nagaya et al. (2008). Triangles and square show F-net and Hi-net stations used in this study, respectively. The Seto Inland Sea is abbreviated as S.I.S.

2. Shear-wave splitting analysis of Ps phases on receiver functions

The P-wave receiver function analysis is applied to teleseismic seismograms recoded at twelve F-net stations and one Hi-net station in the Kinki, Chugoku, Shikoku and Kyushu districts, southwest Japan (see Fig. 1). The station locations are listed in Table 1. The F-net and Hi-net are seismic networks deployed over Japan by National Research Institute for Earth Science and Disaster Prevention. The F-net stations are equipped with STS-1 or STS-2 type broadband velocity seismometer. The Hi-net stations are set up with short-period velocity seismometer. The F-net waveform data

Table 1
Locations of stations and values of splitting parameters.

Station code	Latitude	Longitude	ϕ_s (°)	δt (s)	N
ABU	34° 51′ 49″	135° 34′ 14″	16 ± 3	0.64 ± 0.23	30
BSI	34° 40′ 47″	133° 34′ 25″	−24 ± 2	0.17 ± 0.07	37
INN	33° 28′ 12″	131° 18′ 22″	−78 ± 2	0.12 ± 0.06	18
ISI	34° 3′ 38″	134° 27′ 19″	−85 ± 3	0.13 ± 0.09	28
MNO	34° 11′ 53″	133° 42′ 29″	35 ± 3	0.49 ± 0.00	29
NOK	34° 9′ 56″	135° 20′ 52″	88 ± 14	0.05 ± 0.00	11
NRW	34° 46′ 6″	133° 31′ 57″	−36 ± 3	0.71 ± 0.16	28
NSK	34° 20′ 25″	132° 0′ 6″	20 ± 15	0.73 ± 0.08	18
OKD	34° 41′ 32″	133° 55′ 9″	25 ± 3	0.86 ± 0.08	40
SBR	33° 30′ 19″	130° 18′ 18″	66 ± 14	0.14 ± 0.08	22
TGW	33° 58′ 24″	132° 55′ 54″	67 ± 1	0.26 ± 0.28	23
TKD	32° 49′ 4″	131° 23′ 15″	−76 ± 1	0.05 ± 0.00	14
TMC	32° 36′ 23″	130° 54′ 54″	−75 ± 10	0.46 ± 0.26	32
TSA	33° 10′ 41″	132° 49′ 12″	−66 ± 3	0.10 ± 0.06	19
UMJ	33° 34′ 46″	134° 2′ 12″	−10 ± 4	0.21 ± 0.31	21
YAS	35° 39′ 25″	135° 9′ 37″	−67 ± 2	0.77 ± 0.07	31
YSI	35° 11′ 39″	132° 53′ 10″	55 ± 3	0.10 ± 0.05	24
YTY	34° 17′ 1″	131° 2′ 11″	−76 ± 0	0.17 ± 0.06	22
YZK	35° 5′ 20″	134° 27′ 33″	−4 ± 3	0.13 ± 0.11	20

ϕ_s is the fast polarization direction measured clockwise from the north.
N denotes the number of ϕ_s data used to make rose diagram.

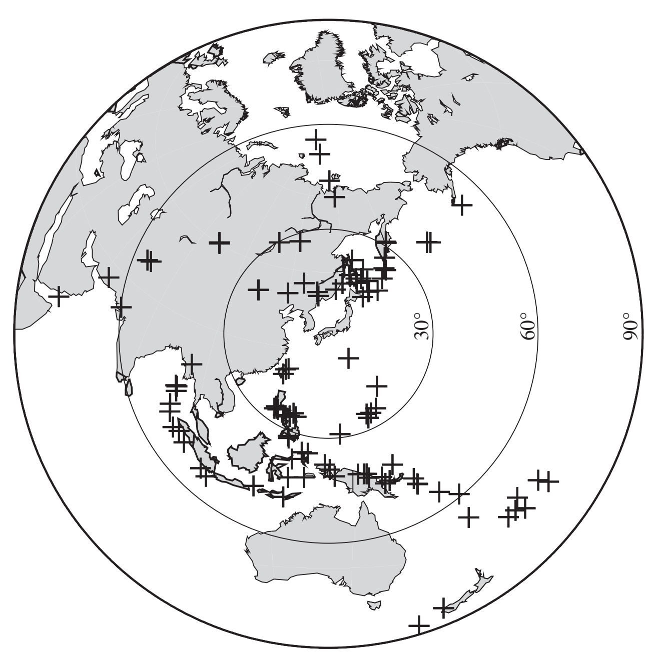

Fig. 2. Locations of earthquake epicenters (cross) used in this study. Epicentral distances of 30°, 60° and 90° are shown by circles.